УДК:550.38:550.385 DOI: https://doi.org/10.24028/gj.v47i3.323184

Spatio-temporal disturbances of the Earth's magnetic field along the Struve Geodetic Arc

M.I. Orlyuk, A.O. Romenets, A.V. Marchenko, I.M. Orliuk, 2025

S. Subbotin Institute of Geophysics of National Academy
of Sciences of Ukraine, Kyiv, Ukraine
Received 18 February 2025

In 1816—1855, astronomer Friedrich Georg Wilhelm von Struve made the first topographic measurements along a 2822 km-long segment of the meridian stretching from northern Norway (70°40′N) to southern Odesa Region (45°19′N). Struve wanted to determine the exact size and shape of the planet. This segment is a good testing ground for studying the geomagnetic aspect of solar-terrestrial interactions, as both the main magnetic field of the Earth and the anomalous magnetic field at surface and ionospheric heights change significantly within its boundaries. The article studies the magnetic storm on May 10—13, 2024 given the module and anomalies of the geomagnetic field induction module along the Struve Geodetic Arc. To characterize the Earth's internal magnetic field, digital maps of the induction module and anomalies at heights of 4 and 100 km were developed. For the magnetic storm, observations of variations in the northern, eastern, and vertical components of the geomagnetic field induction module at 7 magnetic observatories were used. For each observatory, we calculated the induction modulus of the internal magnetic field B_{int}, the modulus of the main magnetic field (core field) B_{IGRF}, the amplitude and mean value of the geomagnetic field variation, and the variation of the parameter ΔD, which reflects the ratio of the anomaly of the geomagnetic field induction modulus to the B_{IGRF} field. The amplitude of the geomagnetic field variations and their average values depended on the modulus of the main magnetic field of the Earth B_{IGRF} ($R^2_{\delta B/B_{\text{IGRF}}} = 0.96$ and $R^2_{\delta B_{\text{average}}/B_{\text{IGRF}}} = 0.7$, respectively). The dependence naturally increases with latitude, from 265 nT (SUR) and 457 nT (ODE) to 1502 nT (NUR) and 2408 nT (SOD). A slightly lower correlation was observed for the B_x component of the geomagnetic field and B_{IGRF} ($R^2_{\delta B_x/B_{\text{IGRF}}} = 0.89$). The amplitude of variation of the spatio-temporal disturbance of the geomagnetic field $\delta(\Delta D)$ also correlates highly with the B_{IGRF} module ($R^2_{\delta(\Delta D)/B_{\text{IGRF}}} = 0.96$). The pattern is confirmed by a stronger manifestation of the magnetic storm on May 10—13, 2024 and a shift of its maximum disturbances by 4 degrees to the south compared to the storm of November 29—31, 2003, during which the B_{IGRF} field induction module for the northern part of the Struve Geodetic Arc increased by 830—930 nT. We found a connection between the maximum manifestation of the geomagnetic storm and regional magnetic anomalies on the Earth's surface and their superposition at an altitude of 100 km. The maximum magnitude of the magnetic disturbance is recorded at the Pello station in the region of the maximum anomalous magnetic field (more than 90 nT at an altitude of 100 km), in contrast to the Mikkelvik station in the zone of the minimum geomagnetic field. This is partially confirmed by the variation of ΔB anomalies due to the magnetization of their sources by the variation of the external field. The most probable reason for the connection between the amplitude of external field variations and the modulus of the

Citation: Orlyuk, M.I., Romenets, A.O., Marchenko, A.V., & Orliuk, I.M. (2025). Spatio-temporal disturbances of the Earth's magnetic field along the Struve Geodetic Arc. *Geofizychnyi Zhurnal*, *47*(3), 102—118. https://doi.org/10.24028/gj.v47i3.323184.

main magnetic field of the B_{IGRF} and the anomalous magnetic field ΔB is their effect on the formation of ionospheric currents.

Key words: Earth's internal magnetic field, geomagnetic field variations, Struve Geodetic Arc, ionosphere.

Introduction. At present, the issues of solar-terrestrial interactions are very relevant, especially the mechanisms of transmission of deep space disturbances to the Earth's surface. One of the main components of the solar-terrestrial interactions is the magnetic field. On the one hand, it is a link between the Sun and the Earth, and, on the other hand, causes a different response to the same impact depending on the «relief» of the Earth's internal magnetic field. A number of recent publications have made a reasonable assumption about the influence of the geomagnetic field topography on the nature of processes in the Earth's ionosphere and magnetosphere [Orlyuk, Romenets, 2011, 2020; Cnossen et al., 2012; Chornohor, 2024]. The papers [Orlyuk, Romenets, 2022; Kirov et al., 2022] show a significant connection between the Earth's magnetic field and its changes with the Sun's magnetic field and solar activity. Combined analysis of the Earth's main magnetic field (main field) B_{IGRF} and the Sun's large-scale magnetic field (LSMF) show their regular 11- and 22-year changes, which probably modulate solar activity [Orlyuk, Romenets, 2022]. Meanwhile, the rotating velocity of the two- and four-sector structure of LSMF solar sources varied with approximately 11-year and 22-year cycles [Leiko 2005]. Longer-term changes in the magnetic fields of the Sun and Earth with a period of about 75 years have also been detected [Orlyuk, Romenets, 2023], which coincide with the rotation period of LSMF sources [Obridko et al., 2021] and with the Earth's rotation mode [Lesur et al., 2022]. Given the observed consistency of long-term changes in the large-scale magnetic field of the Sun and the Earth's magnetic field [Orlyuk, Romenets, 2023], as well as the significant dependence of short-term geomagnetic disturbances on solar activity [Kirov et al., 2022], the mechanism of such connection is an important and poorly understood issue. To study this, we investigated the «reaction» of the Earth's magnetic field to the coronal mass ejection of May 7, 2024, which reached the Earth's orbit on May 10, 2024, and the associated magnetic storm that lasted more than 24 hours. This unique space weather event caused a 9-point magnetic storm and, accordingly, the aurora borealis, which was observed at latitudes around 40—30°N. Other consequences included a solar radiation storm, strong radio obscuration, changes in the density of the thermosphere at ionospheric heights, interference with geolocation systems, and minor changes in the altitude of spacecraft and satellites [Elvidge, Themens, 2025; Grandin et al., 2024; Ranjan et al., 2024; Hayakawa et al., 2024]. Currently, the influence of high-energy sources of external origin on magnetospheric-ionospheric processes and related perturbations of the Earth's outer and inner shells is well understood [Olsen, Stolle, 2017; Chornohor, 2021; Usoskin et al., 2023]. The interaction of the magnetospheric-ionospheric geomagnetic disturbance with the Earth's internal magnetic field remains less studied.

We studied the perturbations of the Earth's magnetic field along the meridian of the 2822-km-long Struve Geodetic Arc (SGA) (over 25°). The SGA was measured from 1816 to 1855 from Fuglenes (in the vicinity of Hammerfest near Cape Nordkap, Norway, 70° 40′ 12″ N, 23° 39′ 48″ E) to Staro-Nekrasivka (near Izmail, Odesa region, 45° 19′ 54″ N, 28° 55′ 41″ E). These are the extreme points of the geodetic measurements made by the astronomer Friedrich Georg Wilhelm Struve and his colleagues (the Struve Geodetic Arc — UNESCO World Heritage Center https://whc.unesco.org/en/list/1187/). The SGA meridian is characterized by significant changes in the Earth's main magnetic field (core field) and anomalous magnetic field (lithosphere field). There are 7 magnetic observatories in the vicinity of the SGA, which makes it possible to assess the nature of magnetic storm

on May 10—13, 2024, depending on the global and regional characteristics of the Earth's internal magnetic field.

The paper aims presents the statistical analysis of the course of a 9-point magnetic storm depending on the planetary and regional features of the Earth's internal magnetic field in the vicinity of the SGA meridian**.**

Materials and methods. To determine the relationship between the geomagnetic field

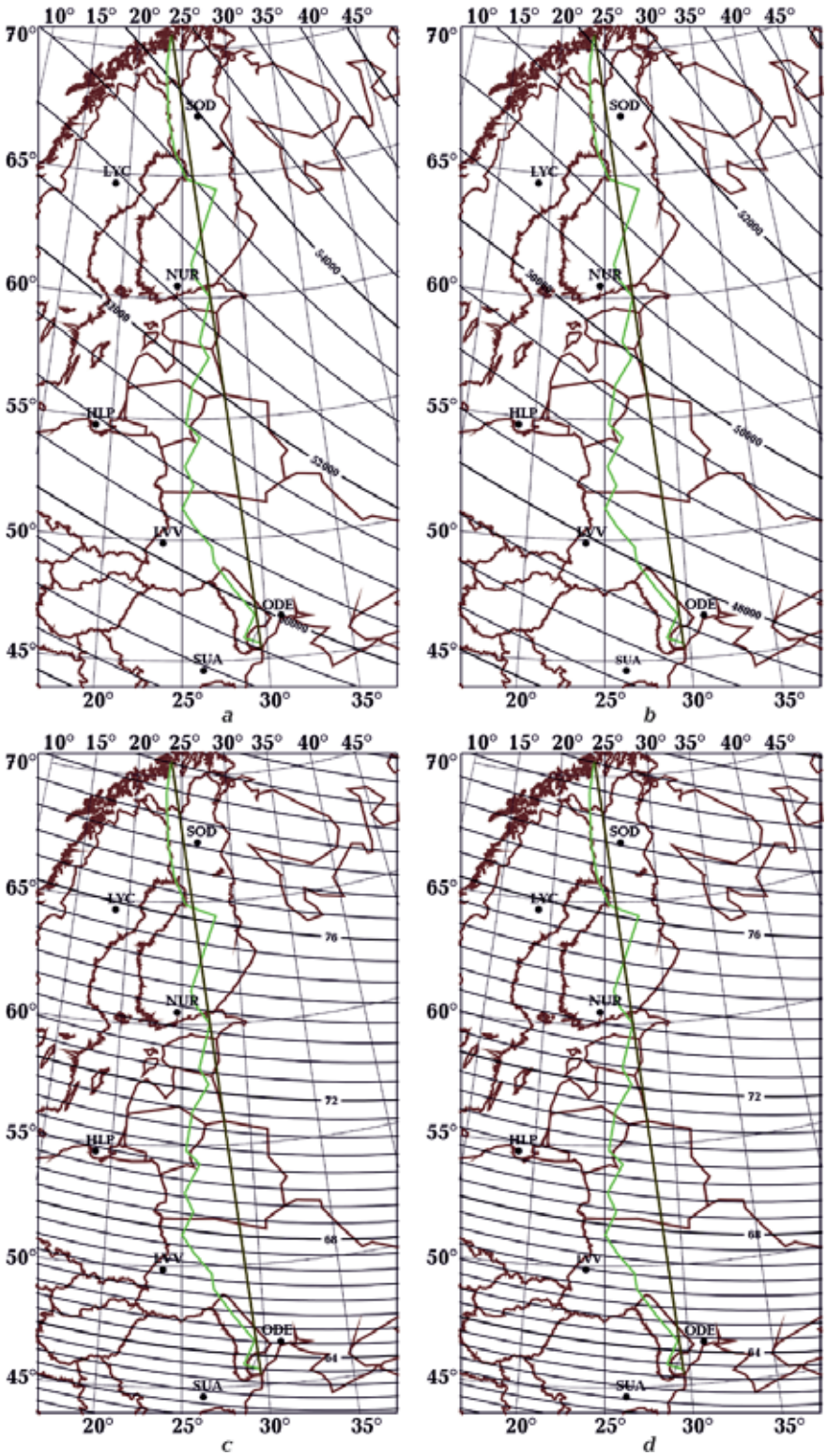

and geomagnetic disturbances caused by solar activity on 10—13.05.2024, we used the DGRF/IGRF model of the Earth's main magnetic field [Brown et al., 2021; Alken et al., 2021], digital maps of the anomalous magnetic field ΔB [Korhonen et al., 2007; Meyer et al., 2017; Liu et al., 2023], the model of the geomagnetic field induction module B [Enhansed ..., 2017], and data of variations of the module B and its components B_x, B_y, B_z from 7 magnetic observatories (https://intermagnet.org/new_data_download.html) in the area of the SGA meridian. The observed geomagnetic field induction modulus consists of the sum of its normal, anomalous and variational components $B=B_{IGRF}+\Delta B+\delta B$. The internal magnetic field is the sum of the main (core) and anomalous (lithosphere) fields $B_{int}=B_{IGRF}+\Delta B$. High-frequency variations of the geomagnetic field δB are determined by both magnetospheric-ionospheric currents and induced currents in the magnetic and electric inhomogeneities of the Earth's lithosphere and mantle [Rokityansky, Tereshyn, 2024]. To determine this component of the geomagnetic field δB (or its components δB_x, δB_y, δB_z) in a separate observatory, it is proposed to calculate it using the formula $\delta B=B_{obs}-(B_{IGRF}+\Delta B)$. The calculation of the geomagnetic field components is performed according to the same principle $\delta B_i=B_{obs,i}$ $(B_{IGRF,i}+\Delta B_{int})$, where $i=x, y, z$. The spatial and temporal perturbation of the geomagnetic field induction module is estimated by the formula: $\Delta D=((B_{obs.}-B_{int})/2B_{IGRF})\cdot 10^5$. The interpretation of the raw data was carried out according to standard methods. It was reduced to the calculation of the modulus of induction of the Earth's magnetic field and its normal and anomalous components at the Earth's surface and at heights of 4 and 100 km, and to the selection and analysis of variations in the geomagnetic field of the observatories in relation to their amplitudes and periods. Finally, we analyzed the relationship between

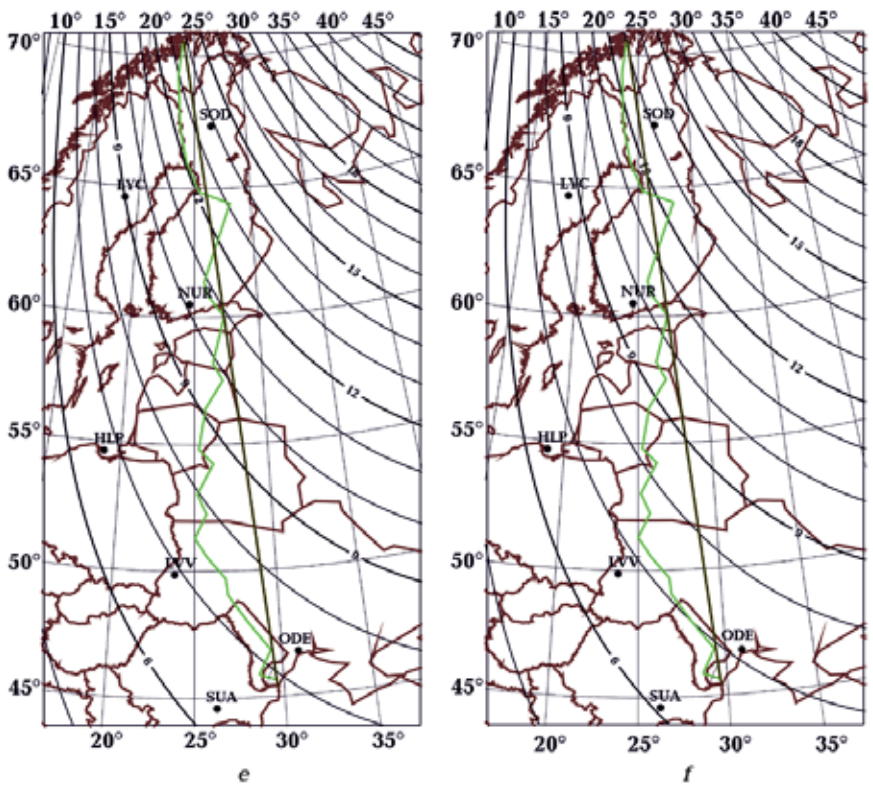

Fig. 1. The Earth's main magnetic field B_{IGRF} at an altitude of 4 km (*a*) and 100 km (*b*), inclination I (*c* and *d*) and declination D (*e* and *f*), respectively. Field isodynes in nanotesla, isolines I and D in degrees. Contours of countries and coastlines are brown solid lines. Black dots and captions show the locations and names of observatories: Sodankyla (SOD: 67.37°N, 26.63°E), Lycksele (LYC: 64.612°N, 18.748°E), Nurmijarvi (NUR: 60.51°N, 24.66°E), Hel (HLP: 54.6035°N, 18.8107°E), Lviv (LVV: 49.90°N, 23.75°E), Odesa (ODE: 46.783°N, 30.883°E), Surlari (SUR: 44.68°N, 26.25°E).

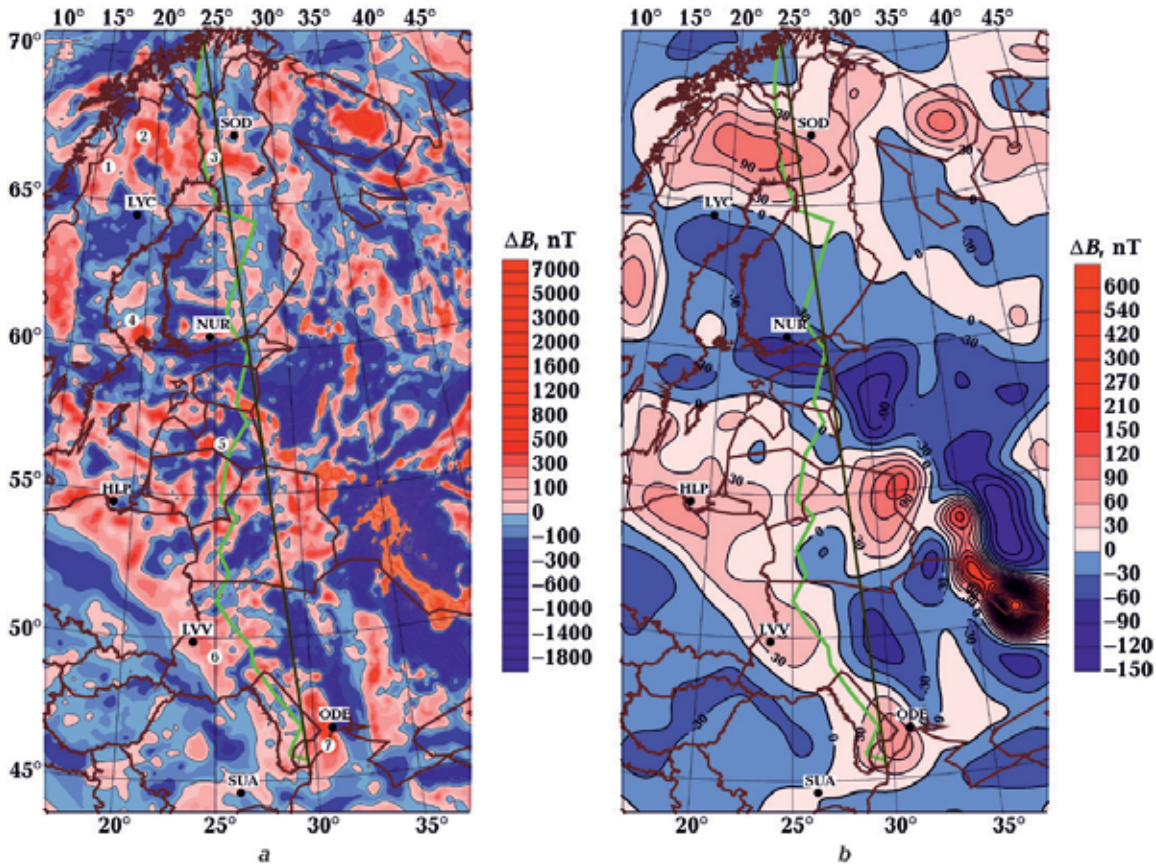

Fig. 2. Anomalous magnetic field Δ*B* at altitudes of 4 km (*a*) and 100 km (*b*). Field isolines and the intensity scale are in nanoteslas. The numbers in white circles are the names of regional magnetic anomalies: 1 — Nurlan, 2 — Kirun, 3 — Lapland, 4 — South Bothnia, 5 — Riga, 6 — Lviv, 7 — Odesa. Others conventional signs see in Fig. 1.

magnetic variations and the modulus of the Earth's normal magnetic field and regional features of the anomalous magnetic field at near-surface and ionospheric heights.

The Earth's internal magnetic field. The shape and distribution of the Earth's magnetosphere is determined by its internal magnetic field, namely the field of its core and lithosphere. In the vicinity of the SGA meridian, these fields vary significantly with latitude (B_{IGRF} field) and the magnetization of lithospheric rocks (Δ*B* field). The induction modulus of the B_{IGRF} field varies from 49500 T in the south to 54500 T in the north. The inclination and declination of the vector on the Earth's surface change from *I*=62.8°, *D*=6.9° in the south to *I*=78.8°, *D*=13.8° in the north. At an altitude of 100 m, the B_{IGRF} field modulus varies from 47.000 nT in the south to 52.000 nT in the north. The inclination and declination of the vector change from *I*=62.6°, *D*=6.7° in the south to *I*=78.8°, *D*=13.1° in the north (Fig. 1).

Anomalous magnetic field ΔB. The magnetic field of the lithosphere has a rather differentiated character with the presence of positive and negative anomalies, which are combined into peculiar lines of predominantly northwestern direction (Fig. 2). The intensity of the anomalies on the Earth's surface varies within ±(400—800) nT. At the same time, there are positive regional magnetic anomalies with transverse dimensions up to 100 km caused by sources in the Earth's lithosphere at depths of 10—50 km [Orlyuk, 2000; Orlyuk et al., 2017].

According to [Orlyuk, 2000; Orlyuk et al., 2017], a number of regional magnetic anomalies are distinguished in the studied area, namely: Nurlan, Kirun, Laplan, South Bothnia within the Baltic Shield and Riga, and Lviv and Odesa in the southwestern part of

Table 1. Parameters of the geomagnetic field induction modulus B, its normal B_{IGRF} and anomalous ΔB components at the Earth's surface and altitudes of 4 and 100 km for 2024

Observatory	SUA	ODE	LVV	HLP	NUR	LYC	SOD
Latitude, deg.	44.68	46.776	49.9	54.60	60.51	64.612	67.37
Longitude, deg.	26.25	30.9	23.75	18.81	24.66	18.748	26.63
B_{-2024}, nT	48854	49925	50355	50769	52723.8	52670	53285
$B_{IGRF-2024}$	48947	50034	50177	50902	52587	52906	53958
ΔB_{-4km}	–2.7	25.1	152.6	–0.9	102.8	–125.6	8.1
$B_{IGRF-4km-2024}$	48935	50037	50182	50925	52594	52914	53970
$B_{-4km-2024}$	48932	50062	50335	50925	52696	52788	53978
ΔB_{-100km}	1.3	45.8	47.7	55	–56	–27.2	49
$B_{IGRF-100km-2024}$	46651	47732	47914	48691	50354	50712	51731
$B_{-100km-2024}$	46652	47778	47961	48746	50298	50685	51780

the East European Craton. The transformed magnetic field of the lithosphere at a height of 100 km varies within ±(60—100) nT.

The anomalous magnetic field at this height is caused by the superposition of regional class sources and is characterized by the presence of low-intensity positive and negative anomalous bands of the northwestern direction (see Fig. 2). The total geomagnetic field both on the Earth's surface and at heights of 4 and 100 km shows both planetary and regional features of its changes [Orlyuk et al., 2024a,b]. The SOD, HLP, LVV, and ODE observatories are located in the zones of positive anomalies, and the NUR and SUR observatories are located in the zones of negative ones.

The Earth's variation magnetic field. To analyze the variation of thegeomagnetic field, we used data from 7 magnetic observatories at different latitudes in the vicinity of the SGA meridian (Table 1). At the same time, the observatories are located atdifferent geographical and geomagnetic latitudes, which allows obtaining reliable information on changes in the nature of the geomagnetic disturbance depending on the planetary and regional features of the geomagnetic field on the Earth's surface and ionospheric heights.

Various local and planetary indices (D_{st}, K_i, K_p, *aa*, *am*, *an*, *as*) are used to estimate the geomagnetic field perturbation caused by the magnetospheric-ionospheric equatorial and auroral electric currents. The indices are calculated by averaging or sampling with a certain time interval of the observed field [Loewe, Prölss, 1997; Menvielle et al., 2010; Chambodut et al., 2015; Matzka et al., 2021; Yamazaki et al., 2022]. The baseline for assessing the geomagnetic field disturbance is the value of its variation on calm days B_{Sq} [Kieokaew et al., 2024]. As that the geomagnetic field disturbance indices lead to its simplification, we used digital data of the geomagnetic field variations and its northern B_x, eastern B_y, and vertical B_z components with a 1-minute sampling. Fig. 3 shows the variations of the geomagnetic field induction B as the most general parameter of its perturbation as well as the scalar of its northern component B_x.

To characterize the induction modulus of geomagnetic field variation, we used its amplitude defined as the difference between the maximum and minimum values of the geomagnetic perturbation and its average value as the sum of 1-minute values during the storm (Table 2). The field level was determined by the modulus of induction of the Earth's internal magnetic field at the time interval before the start of the magnetic storm.

According to the calculations, the amplitude of the northern δB_x component of geomagnetic field variation varies within 657—3607 nT, the eastern δB_y within 522—2234 nT, the vertical δB_z within 243—2465 nT, and the δB module within 265—2408 nT. At the same

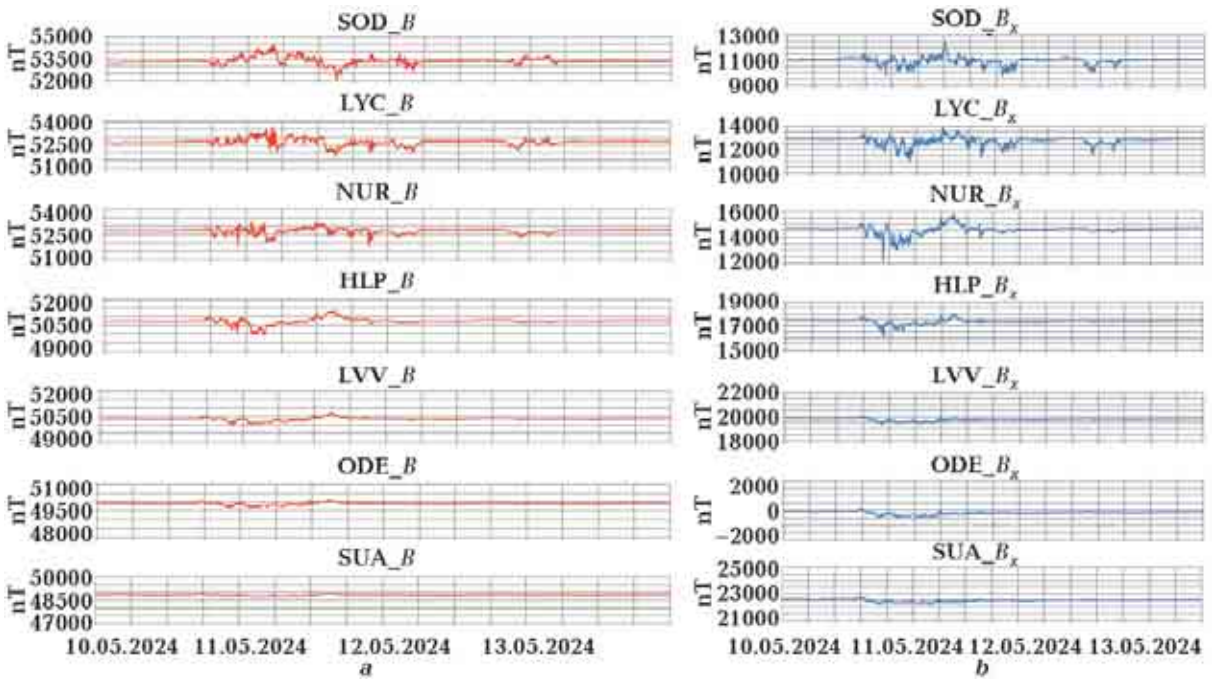

Fig. 3. Induction modulus of the geomagnetic field B (*a*) and its northern component B_x (*b*) in the observatories for the time interval 10.05.2024—13.05.2024.

Table 2. Characteristics of geomagnetic disturbance in magnetic observatories

Observatory	B_{min}, nT	B_{max}, nT	δB_{min}, nT	δB_{max}, nT	$A_{B max - B min}$, nT	$\delta B_{average}$, nT
SUA	48704.94	48970.62	–149.13	116.55	265.68	–24
ODE	49670.57	50127.628	–248.61	208.45	457.06	–17.1
LVV	50004.19	50693.938	–340	350	689.74	–13.9
HLP	49951.9	51365.8	–817.22	596.68	1413.9	–28.55
NUR	51782.48	53284.775	–941.34	560.96	1502.29	–27.05
LYC	51789.7	53671.2	–880.57	1000.93	1881.5	7.93
SOD	52044.18	54452.499	–1240.97	1167.35	2408.31	85.81

time, a natural increase in the maximum amplitude of variation from south to north is characteristic only of the northern component and the geomagnetic field induction module. The maximum value of the δB_x component was recorded at the NUR Observatory, and the δB_y component at the LYC Observatory.

The correlation of variations of δB_x, δB_y, δB_z, and δB with the B_{IGRF} module shows that the greatest correlation is found for the vertical component of the geomagnetic field and the induction module (Fig. 4).

For further analysis of the interaction of external and internal geomagnetic fields in the SGA band, we used variations of the geomagnetic field induction modulus and its northern component and the modulus of the Earth's main magnetic field B_{IGRF}, as they are maximally correlated with each other.

The calculations show that as the B_{IGRF} module increases from south to north, the amplitude of the difference between the maximum and minimum values of the induction module B and its variation δB during the magnetic storm also naturally changes: from 265 nT (SUR) and 457 nT (ODE) to 1502 nT (NUR) and 2408 nT (SOD) (see Table 2, Fig. 5). The significant correlation between the maximum amplitude of the variation field (δB) and the normal magnetic field of B_{IGRF} ($R^2_{B_{max}-B_{min}/B_{IGPH}} = 0.96$) is also characteristic of the calculated average value of the variation of $\delta B_{average}$ in each observatory ($R^2_{\delta B_{average}/B_{IGRF}} =$ $=0.7$). In this case, at the latitude of the Nur-

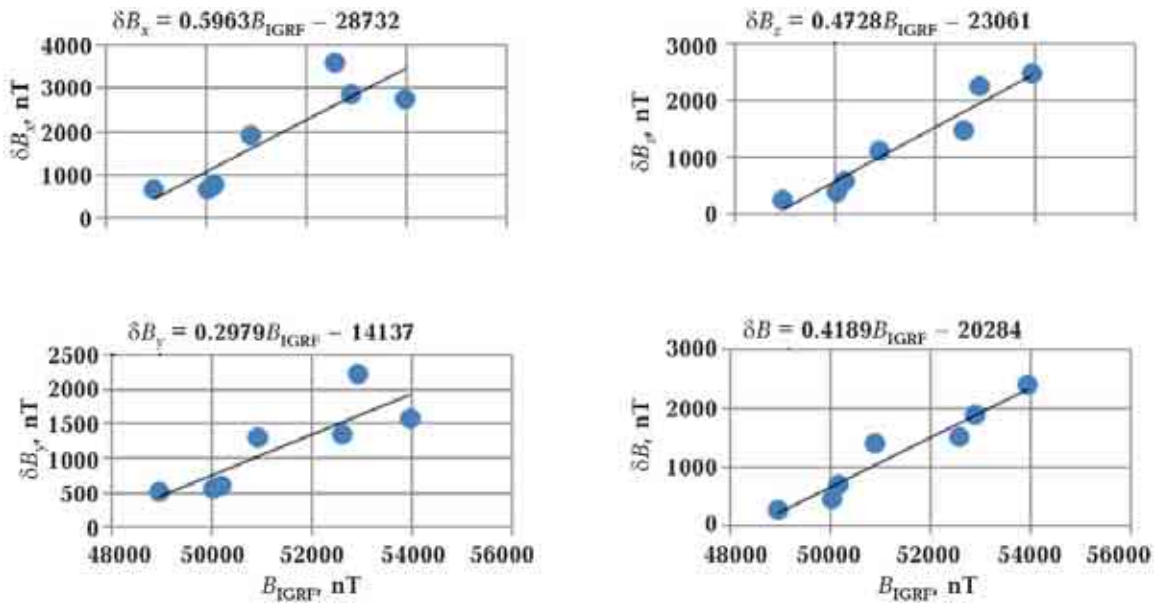

Fig. 4. Correlation of variations of the northern δB_x, eastern δB_y, and vertical δB_z components of the geomagnetic field and its induction module δB of the geomagnetic field with the B_{IGRF} module. $R^2_{\delta B_x/B_{\mathrm{IGRF}}} = 0.89$; $R^2_{\delta B_y/B_{\mathrm{IGRF}}} = 0.84$; $R^2_{\delta B_z/B_{\mathrm{IGRF}}} = 0.97$; $R^2_{\delta B/B_{\mathrm{IGRF}}} = 0.96$.

miyarvi magnetic observatory, the phase and average values of the geomagnetic field induction change during the course of the magnetic storm. South of the Nurmiyarvi Observatory the magnetic storm is characterized by a change in the phase and average values of the geomagnetic field induction during the course of the storm. Nurmiyarvi is characterized by a negative phase and negative mean values of geomagnetic field variations, and to the north — by their positive values (see Fig. 3, *a* and Table 2).

The northern component of the geomagnetic field modulus B_x variation is in-phase along the entire SGA meridian (see Fig. 3, *b*). In this case, as well as for the variation of the geomagnetic field induction module, there is a significant correlation between the

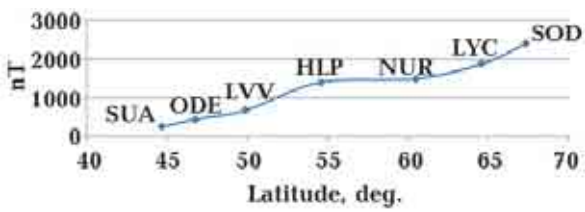

Fig. 5. Variation of the maximum amplitude of the geomagnetic field variation according to the latitude of observatory.

B_x component and the normal B_{IGRF} field ($R^2_{\delta B_x/B_{\mathrm{IGPH}}} = 0.89$).

To assess the possible manifestation and influence of regional magnetic field features on the history of ionospheric processes, we analyzed the amplitude of variations field δB and their average values based on observational data with *B*-module anomalies directly at the Earth's surface and at altitudes of 4 and 100 km (see Tables 1 and 3). Formal analysis of the correlation dependencies shows that there is no connection between magnetic perturbation and the anomalous magnetic field at different altitudes. However, the peak minimum of the average value of the induction modulus variation ($\delta B_{\mathrm{average}} = -28$ nT) falls on the Nurmiyarvi Observatory, which is located in the region of the regional minimum of the magnetic field (see Fig. 2, *b*). It should be noted that the maximum perturbations of the northern component of the geomagnetic field B_x during the magnetic storm of May 10—13, 2024 were also recorded at this observatory [Kärhä et al., 2024].

The data on the assessment of the spatial and temporal perturbation of the geomagnetic field during a magnetic storm using the new ΔD criterion are given in Table 3 and

Fig. 6. According to the calculations, the amplitude of the space-time disturbances of the geomagnetic field δ(Δ*D*) naturally increases depending on the latitude of the observatory, from 273 Dist at the SUA observatory to 2240 Dist at the SOD observatory (see Table 3, Fig. 6, *a*).

The geomagnetic field induction modulus of the B_{IGRF} increases from south to north along the SGA meridian with the same pattern, from 48947 nT at SUA to 53958 nT at SOD (see Table 3, Fig. 3, *b*). The calculated correlation between the amplitude of variation of the geomagnetic field space-time perturbation δ(Δ*D*) and the magnitude of the B_{IGRF} field is significant, R^2=0.96 (see Fig. 3, *b*). Taking into account the standard deviation, which differs from the general pattern for HLP, which is located far from the SGA meridian (see Figs. 1, 2), we calculated the dependence of δ(Δ*D*) and B_{IGRF} without this observatory (R^2=0.99).

Discussion. The analysis of the geomagnetic field *B* variation, its northern component B_x, and the parameter Δ*D* during the magnetic storm showed their strong dependence, first of all, on the induction modulus of the main magnetic field B_{IGRF}. This can certainly indi-

Table 3. Characteristics of the disturbance Δ*D* of the geomagnetic field (dimensionless quantity) in magnetic observatories

Observatory	ΔD_{min}	ΔD_{max}	Amplitude δ(Δ*D*)	Standard deviation, σ	B_{IGRF_2024}
SUA	–42.23	230.3	272.53	40.68	48947
ODE	–166.58	291.98	458.56	53	50034
LVV	–511.77	178.06	689.83	76.46	50177
HLP	–774.37	618.97	1393.34	149.28	50902
NUR	–607.9	825.05	1432.95	131.04	52587
LYC	–900.74	883.01	1783.75	179.64	52906
SOD	–1593.38	646.61	2239.99	206.74	53958

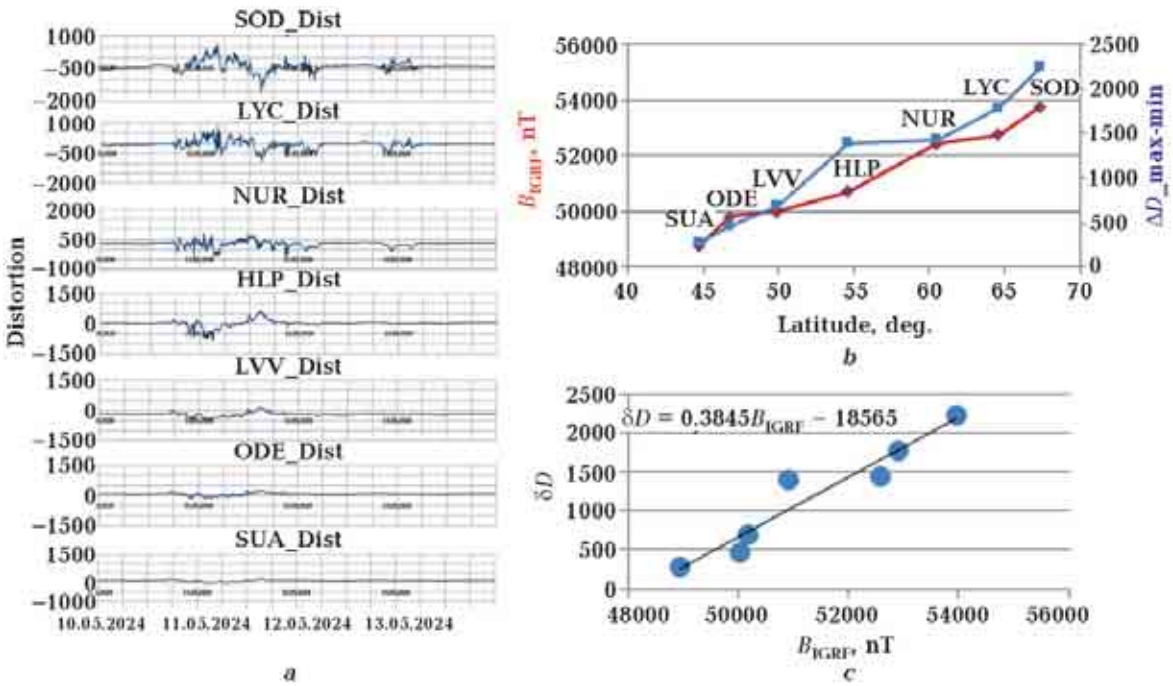

Fig. 6. Spatio-temporal disturbances of the geomagnetic field in the vicinity of the SGA meridian: *a* — variations of δ(Δ*D*)·10^{-5} for observatories, *b* — comparison of the δ(Δ*D*)·10^{-5} amplitude with the B_{IGRF} value, *c* — correlation between the δ(ΔD)·10^{-5} amplitude and the B_{IGRF} (regression equation δ(Δ*D*)=0.3845 B_{IGRF}–18565).

cate a strong modulating role of the Earth's internal magnetic field in the formation of magnetospheric-ionospheric currents and, accordingly, in the variation of the external field. The potential influence of the B_{IGRF} field on the amplitude of the external field variation can be confirmed by experimental data on the Mother's Day storm and the Halloween storm [Kärhä et al., 2024]. The strongest perturbations of the magnetic north (B_x) component during the Mother's Day storm of 2024 occurred at the Nurmijärvi station (NUR: 60.50°N, 24.65°E), and the strongest perturbations of this component during the Halloween storm of 2003 occurred at the Oulujärvi station (OUJ: 64.52°N, 27.37°E). Probably, the stronger manifestation of the Mother's Day storm and the displacement of its maximum disturbances by 4 degrees to the south compared to the Halloween storm can be caused by a change in the vector and the B_{IGRF} induction module. The B_{IGRF} field induction modulus for the northern part of the SGA was in the range of 51400—53600 nT for the 2003 epoch and increased by 830—930 nT from 30.10.2003 to 10.05.2024 (Fig. 7, *a*, *b*). During the same period, the magnetic declination D changed within 3.3°—5.0°, and the inclination

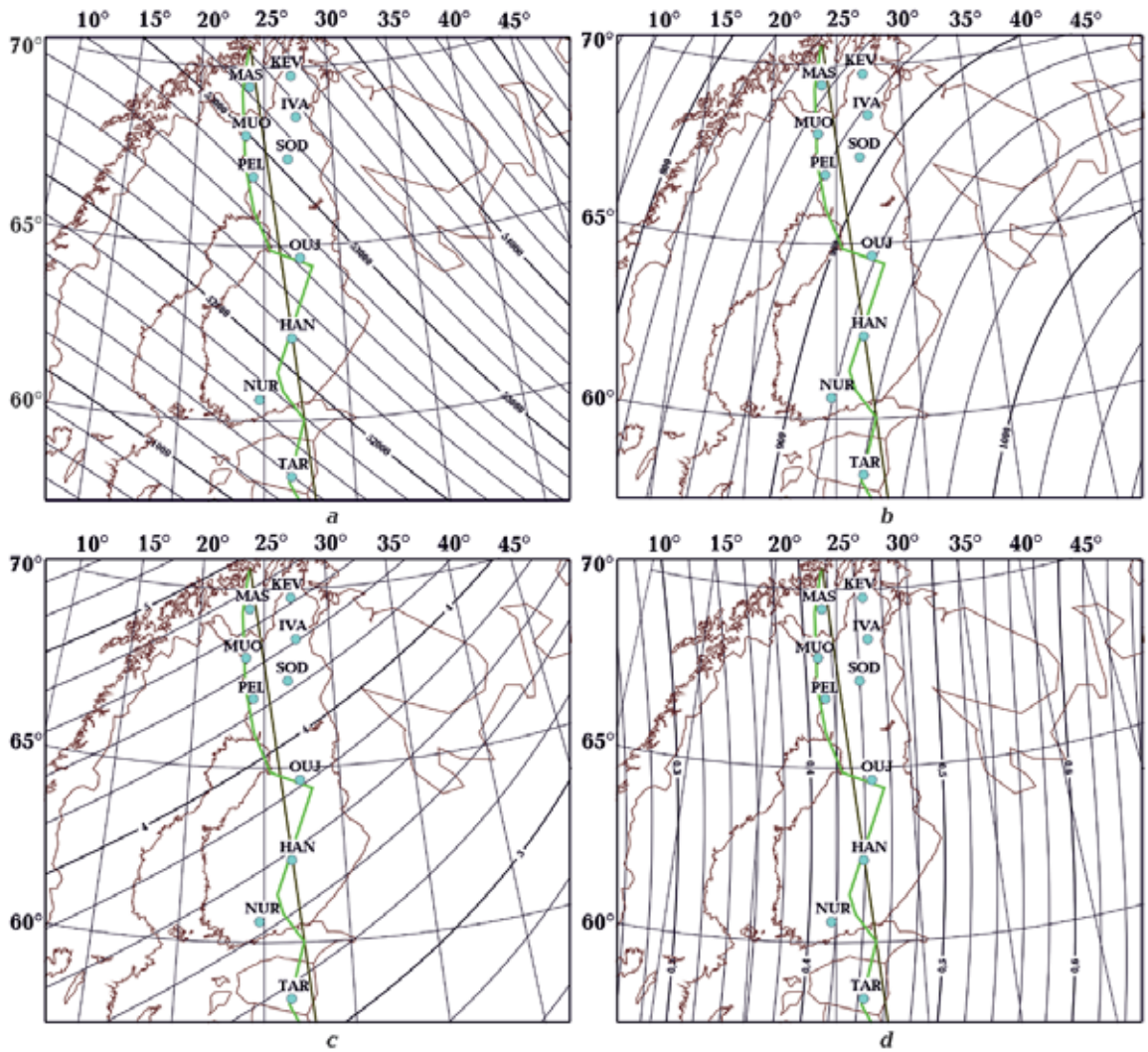

Fig. 7. The Earth's main magnetic field B_{IGRF} induction modulus (*a*), its changes for the period 2003—2024 (*b*), changes in magnetic declination D (*c*) and inclination I (*d*). Magnetometer stations and their geographical coordinates after [Kärhä et al., 2024]: Kevo (KEV: 69.76°N, 27.01°E), Masi (MAS: 69.06°N, 20.77°E), Ivalo (IVA: 68.56°N, 27.29°E), Muonio (MUO: 68.02°N, 23.53°E), Sodankylä (SOD: 67.37°N, 26.63°E), Pello (PEL: 66.90°N, 24.08°E), Oulujärvi (OUJ: 64.52°N, 27.23°E), Hankasalmi (HAN: 62.25°N, 26.60°E), Nurmijärvi (NUR: 60.50°N, 24.65°E), Tartu (TAR: 58.26°N, 26.46°E).

of the field vector I changed by 0.38°—0.46° (Fig. 7, *c*, *d*).

At the same time, the B_{IGRF} module increases in the northeast direction, its change — in the southeast direction, the magnetic declination of the B_{IGRF} vector increases in the northwest direction, and the inclination of D — in the east one.

The influence of regional features of the magnetic field on the variation field is less certain and little studied. It is worth noting that the B_{IGRF} induction modulus at ionospheric heights is threeorders of magnitude larger than the anomalies of the ΔB induction modulus, which can probably explain the lack of correlation between the external variation and the latter. An approximate estimate of the δB variation due to the influence of ΔB anomalies on the ionospheric currents can be made by analyzing the standard deviation from the general pattern in each observatory (see Table 3, Fig. 8).

As can be seen from Fig. 8, the standard deviation relative to its trend component is maximum at the HLP and NUR observatories, which are located at the maximum and minimum of the ΔB field at ionospheric heights, and to a lesser extent at the ODE and LVV observatories. ODE and LVV are located in the marginal parts of the positive anomalies (see Fig. 2). The results of experimental studies and analysis of the B_x component of the D_{st} variation during the storms of October 28, 1977 (D_{st} — 159 nT), December 10—12, 1977 (D_{st} — 112 nT) and the strong storm of October 28—31, 2003 (D_{st} — 353 nT) can serve as a strong confirmation of the potential influence of the regional field on the character of the magnetic storm in the auroral zone [Kärhä et al., 2023]. According to our results, the maximum perturbations in the auroral region occur in the Kiruna and Lapland RMAs and their superposition manifestation at an altitude of 100 km (30—50 nT). In particular, during the magnetic storm of October 30, 2003, the difference in geomagnetic field variations between the Sodankylä Observatory (SOD: 67.37°N, 26.63°E) and Tromso Observatory (TRO: 69.66°N, 19.94°E) reached 1514 nT. At the same time, the SOD observatory is located in region of positive, and TRO — in the region of negative regional magnetic field (Fig. 9). This regularity is also observed for the magnetic storm of December 10—12, 1977, on the example of the geomagnetic field perturbation in the magnetic observatories Mikelvik (MIK: 70.07°N, 19.03°E) and Pelo (PEL: 66.85°N, 24.73°E), which are located at a considerable distance and in a different anomalous field.

In Mikelvik, a westward electric jet caused a perturbation of 215 nT. At Pelo station the perturbation was — 377 nT by an eastward electric jet (see Fig. 1 in [Kärhä et al., 2023]). The maximum magnitude of the magnetic perturbation is recorded at PEL, located in the area of maximum anomalous magnetic field (more than 90 nT at an altitude of 100 km), in contrast to MIK, located in the area of minimum geomagnetic field. The distribution of external currents for the vertical field from the

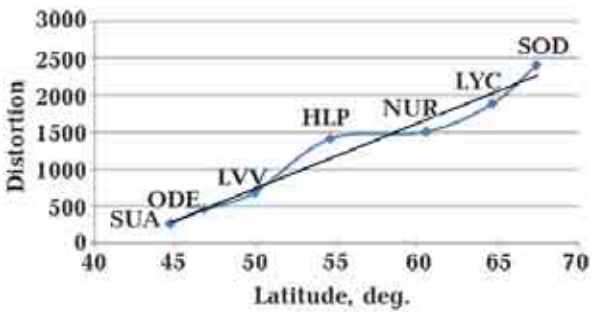

Fig. 8. Standard deviation of geomagnetic field disturbance (blue curve) and its trend (black curve).

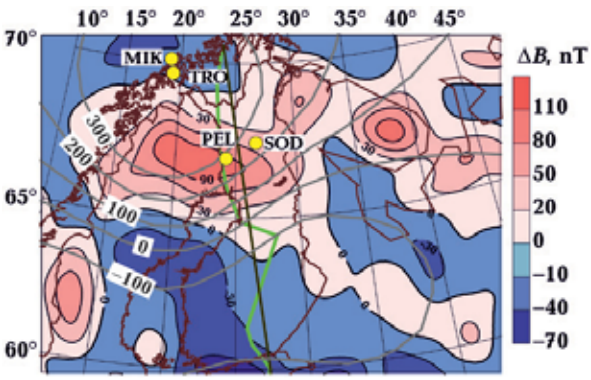

Fig. 9. Anomalous magnetic field ΔB at the 100 km altitude and external current distribution (thick gray lines) for the vertical field (in nT) for the geomagnetic disturbance on June 26, 1998 at 01:18 UT [Pulkkinen et al., 2003]. Locations of magnetic stations (yellow circles).

magnetic disturbance on June 26, 1998 [Pulkkinen et al., 2003] may also, to a first approximation, indicate their certain connection with the anomalous field at an altitude of 100 km. Given the difficulty of separating the geomagnetic field variations into their parts caused by external and internal sources, we estimated the change in ΔB anomalies due to the magnetization of their sources. It is known that in the case of inductive magnetization of rocks of the Earth's crust and upper mantle, the magnitude of the geomagnetic anomaly depends on the field magnetizing the rock [Orlyuk et al., 2024]. The magnetizing field is the B_{IGRF} field, and during magnetic disturbances, the total field, including the external $B_{IGRF}+\delta B_e$ field. Taking into account the proportionality of the ratio of the geomagnetic field anomaly before the disturbance (ΔB_1) and after the disturbance (ΔB_2), the magnetizing field B_{IGRF} and $B_{IGRF}+\delta B_e$ can be calculated relative to the magnetizing field B_{IGRF} and $B_{IGRF}+\delta B_e$, namely $\Delta B_2=(B_{IGRF}+\delta B_e)\cdot\Delta B_1/B_{IGRF}$. The magnitude of the magnetizing effect is estimated by the expression $\Delta\Delta B_{2\text{-}1}=\Delta B_2-\Delta B_1$. According to the calculations for the Lapland anomaly (B_{IGRF}=53000 nT, anomaly intensity on the Earth's surface 700 nT, variation ±1000 nT), the magnitude of the field increase (decrease) in the center of the anomaly will be ±13.2 nT (for a variation of ±2000 nT anomaly ±26.4 nT respectively).

In general, the magnitude of the magnetizing effect for the area of the SGA northern part for a variation of 1000 nT intensity varies from –16 to 56 nT (see Fig. 10). It is natural that the maximum values of this parameter correspond to the maximums and minimums of the anomalous magnetic field ΔB. Very small changes in the geomagnetic field variation are typical for the middle latitudes. In particular, for the Odesa anomaly (B_{IGRF}=50200 nT, anomaly intensity at the Earth's surface=700 nT, variation=±1000 nT), the magnetizing effect is only ±1.9 nT. Thus, during magnetic disturbance, minor changes in variation are possible due to the inductive magnetization of the crustal rocks.

The approach used to assess the geomagnetic field perturbation during a magnetic storm by paying attention of the internal magnetic field B_{int} [Mandea, Chambodut, 2020] (at the time of the magnetic storm) eliminates the need to calculate baselines and allows for a correct analysis of geomagnetic storms of different time. Another important aspect of the study is the use of the parameter ΔD, in which the spatial and temporal variation of the geomagnetic field is normalized by the value of the normal magnetic field B_{IGRF}. This allows us to estimate its value depending on the latitude of the observatory and to analyze it for its connection with regional features of the geomagnetic field at ionospheric heights.

To quantify the predicted impact of regional magnetic anomalies on ionospheric processes and flow specifics of the geomagnetic field variations [Ryabov et al., 2019, 2024; Sukharev et al., 2014, 2022], it is necessary to perform (additionally to the observatory observations) regime observations at the points of the secular course. These points should be located in the areas of regional maxima and minima of the geomagnetic field on the territory of Ukraine, Latvia, Finland and Sweden (see Fig. 2, *b*). Of course, in the future, it will be possible to focus on the Scandinavian Magnetometer Array research (SMA) [Kärhä et al., 2023, 2024], the results of which have already been used in the proposed article to substantiate the connection of the external geomagnetic field perturbations with planetary and regional features of its internal sources. The identified patterns of the rela-

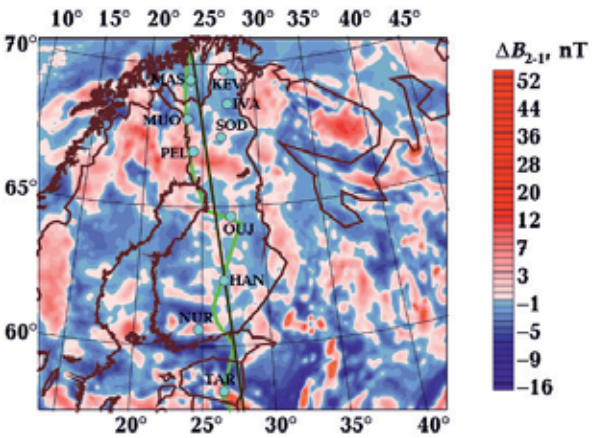

Fig. 10. Map of the magnetizing effect magnitude due to changes in the inductive magnetization of rocks during a magnetic storm with an intensity of 1000 nT.

tionship between geomagnetic variations and the internal geomagnetic field will be further detailed in subsequent research with regard to the nature of individual components and the assessment of their contribution to the total values of geomagnetic disturbance. In particular, in addition to internal sources of the planetary and regional types, a certain contribution to external variation will be determined by the electrical conductivity of various crustal and mantle layers [Pulkkinen et al., 2003]. A comparison of the magnetization and electrical conductivity patterns of the Earth's crust indicates their spatial differences and, accordingly, their different nature; this requires further study and evaluation of their contribution to the overall geomagnetic field disturbance. The patterns of the connection of geomagnetic variations with the internal geomagnetic field will be further studied in detail regarding the nature of individual components and the determination of their contribution to the total values of the geomagnetic disturbance. In particular, in addition to the internal sources of planetary and regional type, a certain contribution to the external variation will be due to the electrical conductivity of various crustal-mantle layers [Pulkkinen et al., 2003]. Comparison of the magnetization and electrical conductivity schemes of the Earth's crust indicates their spatial differences, and thus different nature, which requires their further study and assessment of their contribution to the total disturbance of the geomagnetic field.

Conclusions. Paying attention to the previously found interrelationship of age-related changes of the Earth and the Sun geomagnetic field, this paper considers the geomagnetic aspect of solar-terrestrial connection based on its short-term changes during the magnetic storm on May 10—13, 2024 at 7 observatories located along the Struve Geodesic Arc:

– To characterize the Earth's internal magnetic field, we drew digital maps of module and anomalies of induction module on the Earth's surface, at heights of 4 and 100 km. To characterize the magnetic storm, we used observations of the external geomagnetic field variations for the 7 observatories;

– For each observatory, the induction module of the internal magnetic field B_{int}, the module of the main magnetic field (core field) B_{IGRF}, the maximum amplitude and the average value of the geomagnetic field variation, as well as the parameter ΔD, which reflects the ratio of anomaly of the geomagnetic field induction module to the B_{IGRF} field, were calculated;

– According to the statistical analysis, a significant dependence of the amplitude of external geomagnetic field variations on their average values, as well as the variation of the northern component and the ΔD parameter on the module of the Earth's main magnetic field was found;

– The detected regularity is confirmed by a stronger manifestation of the magnetic storm on May 10—13, 2024 and by the displacement of its maximum perturbations by 4 degrees to the south in comparison with the magnetic storm of November 29—31, 2003. During this time the B_{IGRF} field induction module for the northern part of the SGA increased by 830—930 nT;

– The connection of the geomagnetic storm maximum manifestation with the Earth's surface regional magnetic anomalies and their super positional manifestation at an altitude of 100 km was established;

– The influence of the latter on the formation of ionospheric currents can be considered the most likely mechanism of connection between the amplitude of the external field variations and the Earth's main and lithospheric magnetic fields module.

Acknowledgements. The study was carried out within the framework of the topic «Analysis of the geomagnetic field and magnetic models of lithospheric structures in connection with the solution of geological, geophysical and environmental problems» (State registration number: 0123U100234). The authors of the article thank the employees of the INTERMAGNET network observatories, whose work results contributed to the study, as well as Otto Kärhä and co-authors for the published data obtained on the Scandinavian Magnetometer Array, used to substantiate certain conclusions of the article.

We are especially gratefulto the anonymous reviewers, whose comments and advice significantly improved the final version of the publication.

References

Alken, P., Thébault, E., Beggan, C.D. et al. (2021). International Geomagnetic Reference Field: the thirteenth generation. *Earth, Planets and Space, 73*, 49. https://doi.org/10.1186/s40623-020-01288-x.

Brown, W.J., Beggan, C.D., Cox, G.A., & Macmillan, S. (2021). The BGS candidate models for IGRF-13 with a retrospective analysis of IGRF-12 secular variation forecasts. *Earth, Planets and Space, 73*, 42. https://doi.org/10.1186/s40623-020-01301-3.

Chambodut, A., Marchaudon, A., Lathuillère, C., Menvielle, M., & Foucault, E. (2015). New hemispheric geomagnetic indices α with 15 min time resolution. *Journal of Geophysical Research, 120*(11), 9943—9958. https://doi.org/10.1002/2015JA021479.

Chornohor, L.F. (2021). Physics of geospace storms. *Space Sciences and Technology, 27*(1), 3—77. https://doi.org/10.15407/knit2021.01.003 (in Ukrainian).

Chornohor, L.F. (2024). Statistical characteristics of geophysical fields disturbed by weather fronts. *Space Science and Technology, 30*(3), 80—94. https://doi.org/10.15407/knit2024.03.080 (in Ukrainian).

Cnossen, I., Richmond, A.D., & Wiltberger, M. (2012). Thedependenceofthecoupledmagnetosphere-ionosphere-thermospheresystemontheEarth'smagneticdipole moment. *Journal of Geophysical Research: Space Physics, 117*, A05302. https://doi.org/10.1029/2012JA017555.

Elvidge, S., & Themens, D.R. (2025). The Probability of the May 2024 Geomagnetic Superstorm. *Space Weather, 23*, e2024SW004113. https://doi.org/10.1029/2024SW004113.

Enhanced Magnetic Model (EMM). (2017). Retrieved from https://www.ncei.noaa.gov/products/enhanced-magnetic-model.

Grandin, M., Bruus, E., Ledvina, V.E., Partamies, N., Barthelemy, M., Martinis, C., Dayton-Oxland, R., Gallardo-Lacourt, B., Nishimura, Y., Herlingshaw, K., Thomas, N., Karvinen, E., Lach, D., Spijkers, M., & Bergstrand, C. (2024). The geomagnetic superstorm of 10 May 2024. Citizen science observations. EGU sphere. Preprint. https://doi.org/10.5194/egusphere-2024-2174.

Hayakawa, H., Ebihara, Y., Mishev, A., Koldobskiy, S., Kusano, K., Bechet, S., Yashiro, S. et al. (2024). The Solar and Geomagnetic Storms in May 2024: a Flash Data Report. *The Astronomical Journal, 979*(1). https://doi.org/10.48550/arXiv.2407.07665.

Kärhä, O., Tanskanen, E.I., & Vanhamäki, H. (2023). Large regional variability in geomagnetic storm effects in the auroral zone. *Scientifc Reports, 13*, 18888. https://doi.org/10.1038/s41598-023-46352-0.

Kärhä, O., Tanskanen, EI, & Vanhamäki, H. (2024). Magnetic ground response of the 2024 Mother's Day storm in Northern Europe. *ESS Open Archive.* September 27, 2024. https://doi.org/10.22541/essoar.172745129.97399059/v1.

Kieokaew, R., Haberlel, V., Marchaudon, A., Blelly, P-L., & Chambodut, A. (2024). A novel neural network-based approach to derive a geomagnetic baseline for robust characterization of geomagnetic indices at mid-latitude. arXiv:2410.02311v1 [physics. space-ph]. A preprint. https://doi.org/10.48550/arXiv.2410.02311.

Kirov, B., Georgieva, K., Asenovski, S., Madjarska, M.S., & Dineva, E.A. (2022). Comparison between the Solar Activity in the 11-Year Sunspot Cycles during the Last Two Centennial Solar Activity Minima. A Comparison of the Geomagnetic Activity during the Same Periods. *Proc. of the Fourteenth Workshop «Solar Influences on the Magnetosphere, Ionosphere and Atmosphere» June, 2022* (pp. 87—92). Retrieved from https://spaceclimate.bas.bg/wssozopol/pdf/Proceedings2022.pdf.

Korhonen, J.V., Fairhead, J.D., Hamoudi, M., Hemant, K., Lesur, V., Mandea, M., Maus, S., Purucker, M., Ravat, D., Sazonova, T. & Thébault, E. (2007). *Magnetic anomaly map of the world, scale 1:50,000,000*. Printed by the Geological Survey of Finland. Retrieved from https://ccgm.org/en/product/world-magnetic-anomalies-map-pdf.

Leiko, U.M. (2005). Large-scale magnetic fields of Sun-heliosphere magnetic system. *Spec. Iss. «Kinematika and Fizika Nebesnykh Tel»*, 187—188.

Lesur, V., Gillet, N., Hammer, M.D., & Mandea, M. (2022). Rapid variations of Earth's core magnetic field. *Surveysin Geophysics, 43*, 41—69. https://doi.org/10.1007/s10712-021-09662-4.

Liu, P.F., Jiang, Y., Yan, Q., & Hirt, A.M. (2023). The behavior of a lithospheric magnetization and magnetic field model. *Earth and Planetary Physics, 7*(1), 66—73. http://doi.org/10.26464/epp2023025.

Loewe, C.A., & Prölss, G.W. (1997). Classification and mean behavior of magnetic storms. *Journal of Geophysical Research: Space Physics, 102*(A7), 14209—14213. http://doi.org/10.1029/96JA04020.

Mandea, M., & Chambodut, A. (2020). Geomagnetic Field Processes and Their Implications for Space Weather. *Surveys in Geophysics, 41*(6), 1611—1627. http://doi.org/10.1007/s10712-020-09598-1.

Matzka, J., Stolle, C., Yamazaki, Y., Bronkalla, O., & Morschhauser, A. (2021). The Geomagnetic K_p Index and Derived Indices of Geomagnetic Activity. *Space Weather, 19*(5), e2020SW002641. http://doi.org/10.1029/2020SW002641.

Menvielle, M., Iyemori, T., Marchaudon, A., & Nosé, M. (2010). Geomagnetic indices. In M. Mandea, M. Korte (Eds.), *Geomagnetic observations and models* (pp. 183—228). Springer. http://doi.org/10.1007/978-910-481-9858-0_8.

Meyer, B., Saltus, R., & Chulliat, A. (2017). *EMAG2v3: Earth Magnetic Anomaly Grid (2-arc-minute resolution). Version 3.NOAA National Centers for Environmental Information*. https://doi.org/10.7289/V5H70CVX.

Obridko, V.N., Pipin, V.V., Sokoloff, D., & Shibalova, A.S. (2021). Solar large-scale magnetic field and cycle patterns in solar dynamo. *Monthly Notices of the Royal Astronomical Society, 504*(4). https://doi.org/10.1093/mnras/stab1062.

Olsen, N., & Stolle, C. (2017). Magnetic Signatures of Ionospheric and Magnetospheric Current Systems During Geomagnetic Quiet Conditions — An Overview. *Space Science Review, 206*, 5—25. https://doi.org/10.1007/s11214-016-0279-7.

Orlyuk, M.I. (2000). Spatial and spatio-temporal magnetic models of different-rank structures of the continental-type lithosphere. *Geofizicheskiy Zhurnal, 22*(6), 148—165.

Orlyuk, M.I., & Romenets, A.O. (2022).On the relationship of temporary changes in the Earth's magnetic field with solar activity 19—24 cycles. *Reports of the National Academy of Sciences of Ukraine,* (1), 72—78. https://doi.org/10.15407/dopovidi2022.01.072 (in Ukrainian).

Orlyuk, M.I., & Romenets, A.A. (2020). Spatial-temporal change of the geomagnetic field: environmental aspect. *Geofizicheskiy Zhurnal, 42*(4), 18—38. https://doi.org/10.24028/gzh.0203-3100.v42i4.2020.210670.

Orlyuk, M.I., & Romenets, A.A. (2011). Structure and dynamics of the main magnetic field of the Earth on its surface and in near space. *Odessa Astronomical Publications, 24*, 124—129 (in Ukrainian).

Orlyuk, M.I., & Romenets, A.O. (2023). The Earth's magnetic field and the large-scale magnetic field of the Sun: the solar-terrestrial connection. *Odessa Astronomical Publications, 36*, 172—177. https://doi.org/10.18524/1810-4215.2023.36.290538.

Orlyuk, M., Marchenko, A., & Bakarjieva, M. (2017). 3D magnetic model of the Earth's crust of the Eastern European Craton with the account of the Earth's sphericity and its tectonic interpretation. *Bulletin of the Kyiv National Taras Shevchenko University. Geology, 79*(4), 33—41. https://doi.org/10.17721/1728-2713.79.03.

Orlyuk, M., Marchenko, A., Romenets, A., Bakarzhieva, M., & Orliuk, I. (2024a). Development of geomagnetic field induction module maps for the territory of Ukraine. *Geodynamics, 1*(36), 74—84. https://doi.org/10.23939/jgd2024.01.074.

Orlyuk, M., Romenets, A., Marchenko, A., & Orliuk, I. (2024b). Earth's magnetic field along the «Struve Geodetic Arc». *Abstracts.BLU 2024 — workshop of the Bulgaria-Latvia-Ukraine nitiative for Space Weather Investigations. June 3—7, 2024. Primorsko, Bulgaria.* Retrieved from https://en.venta.lv/initiative-for-space-weather-investigations-2024.

Pulkkinen, A., Amm, O., Viljanen, A., & BEAR Working Group. (2003). Separation of the

geomagnetic variation field on the ground into external and internal parts using the spherical elementary current system method. *Earth, Planets and Space, 55*, 117—129. https://doi.org/10.1186/BF03351739.

Ranjan, A.K., Nailwall, D., Krishna, M.V., Kumar, A., & Sarkhel, S. (2024). Evidence of potential thermospheric overcooling during the May 2024 geomagnetic superstorm. *Journal of Geophysical Research: Space Physics, 129*(12), e2024JA033148. https://doi.org/10.48550/arXiv.2411.14071.

Rokityansky, I.I., & Tereshyn, A.V. (2024). Induction arrow spatial and temporal variations. *Geofizychnyi Zhurnal, 46*(6), 3—40. https://doi.org/10.24028/gj.v46i6.307063.

Ryabov, M., Orlyuk, M., Usoskin, I., Sukharev, A., Bezrukovs, V., & Šteinbergs, J. (2024). Project «Study of space weather events during the 25th solar cycle, observed along the «Struve Geodetic Arc» sector (Ukraine, Latvia, Finland)». *Abstracts. BLU 2024 — workshop of the Bulgaria-Latvia-Ukraine nitiative for Space Weather Investigations. June 3—7, 2024. Primorsko, Bulgaria*. Retrieved from https://en.venta.lv/initiative-for-space-weather-investigations-2024.

Ryabov, M., Sukharev, A., Orlyuk, M., Sobitnyak, L., & Romenets, A. (2019). Comparative analysis of geomagnetic disturbances in the zone of the Odessa magnetic anomaly under different states of solar activity in the 24th cycle. *Radiophysics and Radioastronomy, 24*(1), 68—79. https://doi.org/10.15407/rpra24.01.068 (in Russian).

Sukharev, A.L., Sobitnyak, L.I., Ryabov, M.I., Orlyuk, M.I., Orliuk, I.M., & Romenets, A.A. (2014). Earth's magnetic field dynamics: space weather and solar cycle effect exhibiting. *Odessa Astronomical Publications, 27*(2), 98—100.

Sukharev, A., Orlyuk, M., Ryabov, M., Sobitniak, L., Bezrukovs, V., Panishko, S., & Romenets, A. (2022). Results of comparison of fast variations of geomagnetic field and ionospheric scintillations of 3C 144 radio source in the area of Odessa geomagnetic anomaly. *Astronomical and Astrophysical Transactions, 33*(1), 67—88. https://doi.org/10.17184/eac.6481.

Usoskin, I., Miyake, F., Baroni, M., Brehm, N., Dalla, N., Hayakawa, H., Hudson, H., Timothy, Jull, A.J., Knipp, D., Koldobskiy, S., Maehara, H., Mekhaldi, F., Notsu, Yu., Poluianov, S., Rozanov, E., Shapiro, A., Spiegl, T., Sukhodolov, T., Uusitalo, J., & Wacker, L. (2023). Extreme Solar Events: Setting up a Paradigm. *Space Science Reviews, 219*, 73. https://doi.org/10.1007/s11214-023-01018-1.

Yamazaki, V, Matzka, J., Stolle, C., Kervalishvili, G., Rauberg, J., Bronkalla, O., Morschhauser, A., Bruinsma, S., Shprits, Y., & Jackson, D.R. (2022). Geomagnetic activity index hpo. *Geophysical Research Letters, 49*(10), e2022GL098860. https://doi.org/10.1029/2022GL098860.

Просторово-часові збурення магнітного поля Землі вздовж Геодезичної дуги Струве

М.І. Орлюк, А.О. Роменець, А.В. Марченко, І.М. Орлюк, 2025

Інститут геофізики ім. С.І. Субботіна НАН України, Київ, Україна

У 1816—1855 рр. астроном Фрідріх Георг Вільгельм Струве виконав перші топографічні вимірювання з метою визначення точного розміру і форми планети вздовж сегмента меридіана протяжністю 2822 км, що тягнеться від півночі Норвегії (70°40′N) до півдня Одеської області (45°19′N). Цей сегмент меридіана є добрим полігоном для дослідження геомагнітного аспекту сонячно-земних зв'язків, оскільки в його межах суттєво змінюється як головне магнітне поле Землі, так і аномальне магнітне поле на приземних та іоносферних висотах. У статті викладено результати дослідження характеру протікання магнітної бурі 10—13 травня 2024 р. залежно від модуля та аномалій модуля індукції геомагнітного поля вздовж Геодезичної дуги Струве. Для характеристики внутрішнього магнітного поля Землі розроблено цифрові карти

модуля та аномалій модуля індукції на висотах 4 та 100 км, а для характеристики магнітної бурі використано результати спостережень варіацій північної, східної та вертикальної компонент модуля індукції геомагнітного поля в семи магнітних обсерваторіях. Для кожної обсерваторії розраховано модуль індукції внутрішнього магнітного поля B_{int}, модуль головного магнітного поля (поля ядра) B_{IGRF}, амплітуду та середнє значення варіації геомагнітного поля, а також варіацію параметру ΔD, який відображає відношення аномалії модуля індукції геомагнітного поля до поля $B_{\text{IGRF.}}$ За результатами статистичного аналізу виявлено залежність амплітуди варіацій зовнішнього геомагнітного поля та їх середніх значень від модуля головного магнітного поля Землі B_{IGRF} ($R^2_{\delta B/B_{\text{IGRF}}}=0.96$ та $R^2_{\delta B_{\text{average}}/B_{\text{IGRF}}}=0.7$ відповідно), яка закономірно зростає залежно від широти обсерваторії — від 265 нТл (SUR) та 457 нТл (ODE) до 1502 нТл (NUR) та 2408 нТл (SOD). Трохи менша кореляційна залежність спостережена для B_x компоненти геомагнітного поля та B_{IGRF} ($R^2_{\delta B_x/B_{\text{IGRF}}}=0.89$). Амплітуда варіації просторово-часової збуреності геомагнітного поля $\delta(\Delta D)$ також характеризується високою кореляційною залежністю від модуля B_{IGRF} ($R^2_{\delta(\Delta D)/B_{\text{IGRF}}}=0.96$). Виявлена закономірність підтверджується більш сильним проявом магнітного шторму 10—13 травня 2024 р. та зміщенням його максимальних збурень на 4 градуси на південь порівняно з магнітним штормом 29—31листопада 2003 р., за час між якими модуль індукції поля B_{IGRF} для північної частини Геодезичної дуги Струве збільшився на 830—930 нТл. Виявлено зв'язок максимального прояву геомагнітного шторму з регіональними магнітними аномаліями на поверхні Землі та їх суперпозиційним проявом на висоті 100 км. Максимальна величина магнітного збурення реєструється на станції ПЕЛ, яка розташована в області максимуму аномального магнітного поля (більше 90 нТл на висоті 100 км), на противагу станції МІК, яка розташована у зоні мінімуму геомагнітного поля, що частково підтверджується варіацією аномалій ΔB за рахунок підмагнічування їх джерел варіацією зовнішнього поля. Найбільш вірогідною причиною зв'язку амплітуди варіацій зовнішнього поля з модулем головного магнітного поля B_{IGRF} та аномальним магнітним полем ΔB можна вважати їх вплив на формування іоносферних струмів.

Ключові слова: внутрішнє магнітне поле Землі, варіації геомагнітного поля, Геодезична дуга Струве, іоносфера.